SPIRAL LOADED CAVITIES FOR HEAVY ION ACCELERATION

A. Schempp and H. Klein
Institut für Angewandte Physik
Universität Frankfurt/Main, D6000 Frankfurt/M., FRG

Summary

A transmission line theory of the spiral resonator has been performed and the calculated and measured properties will be compared. Shunt impedances up to 50 MΩ/m have been measured. In a number of high power tests the structure has been tested and its electrical and mechanical stability has been investigated. The static frequency shift due to ponderomotoric forces was between 0.2 and 50 kHz/kW dependent on the geometrical parameters of the spirals. The maximum field strength obtained on the axis was 16 MV/m in pulsed operation and 9.2 MV/m in cw, corresponding to an voltage gain per cavity of up to 0.96 MV. The results show that spiral resonators are well suited as heavy ion accelerator cavities.

Introduction

During the work on slow wave structures for use in linear heavy ion accelerators spiral loaded cavities for very low energies (frequency ≈ 15 MHz, $\beta < 1$ %) were studied in Frankfurt in 1968. Since these spirals with their tubing lengths of about 5 m were too unstable, this investigation had been stopped. New work on this structure was started after 1973 when it was proposed as postaccelerator structure[1-4] for higher particle energies at frequencies of about 100 MHz allowing spirals with relatively short and stiff tubing.

A schematic drawing of a spiral loaded cavity is shown in fig. 1. The spiral is excited to λ/4-oscillations with the maximum voltage on the drift tube. Properly choosing the drift tube dimensions and the rf-phase an ion can gain up to two times the voltage between the spiral drift tube and the tank end plates. The spiral is perpendicular to the beam axis and the change of the field distribution between the drift tubes caused by a change in spiral parameters is neglectable. Therefore spiral and drift tube geometry can be optimized independently. We developed a model to describe the properties of such spiral resonators and to allow a systematic optimization[5]. Besides this we have done a great number of low power level measurements to prove the theory and of high power tests to study ponderomotoric effects and to improve the construction of our single spiral loaded cavities for applications as heavy ion postaccelerator, buncher and rebuncher cavities.

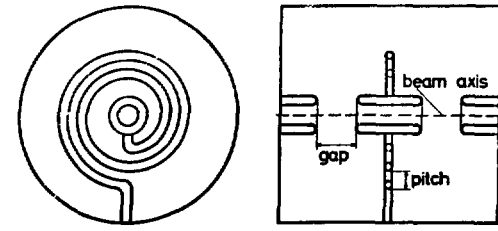

Fig. 1
Schematic drawing of the spiral resonator

Theory and low power level experiments

The spiral resonator is assumed to be an Archimedian spiral with constant pitch s in the cross-section plane of a cylindrical cavity which is closed with end plates. A modified transmission line theory based on the theory for short helices[6,7] is used to calculate the current I and the voltage U along the spiral tubing. The induction law leads to the change in voltage induced in one winding of length $l = 2\pi r$

$$\frac{\partial U}{\partial r} = -\frac{1}{s}\frac{\partial \Phi}{\partial t}$$

A continuity equation follows from the displacement currents to adjacent windings and end plates:

$$\frac{\partial I}{\partial r} = -\frac{1}{s}\frac{\partial}{\partial t}\left(C_0 r U - K_0 r s^2 \frac{\partial^2 U}{\partial r^2}\right)$$

Considering the skin effect a relation between the magnetic flux ϕ and the current I is obtained from the flux distribution between the windings and between spiral and tank end plates.

$$I = \frac{1}{r}\left(\frac{2s}{\mu_0 \pi L}\phi - \frac{s^2 K_0}{\mu_0 4\pi^2}\frac{\partial^2 \phi}{\partial r^2}\right)$$

The capacities C,K between two windings ($C = C_0 \times r$) and between one spiral winding and the end plates ($K = K_0 \times r$) must be inserted for the different tubing cross sections.

These equations can be solved only numerically, for example with help of a Runge-Kutta method. Boundary conditions are the grounding point on the outer conductor and the termination on the axis (r = 0) by a capacity replacing the drift tube.

The lowest mode is similar to a λ/4-oscillation. Fig. 2 shows the voltage and current distribution along the spiral tubing. The measurements were done by bead perturbation method using disc and needle shaped probes [8].

For the shunt impedance η the following definition is used

$$\eta = \frac{4U_M^2}{N \cdot L}$$

U_M, the maximum voltage on the drift tube, is obtained by integrating the peak electrical field E_z along the beam axis of the resonator of length L.

$$U_M = \frac{1}{2} \int_0^L |E_z| \, dz$$

For the calculation of the power loss N the current enhancement between the spiral windings is considered in a way similar to the method used for helices [9] (losses in the outer conductor are neglected). The transit time factor is not considered in this definition of shunt impedance, because as mentioned above, spiral optimization is in practice independent of the drift tube arrangement which can be optimized separately. Figs. 3 and 4 illustrate for some examples the parameter dependance of the shunt impedance. In fig.3 the shunt impedance η of spirals as function of the pitch s is shown. The curves in fig. 4 show the shunt impedance as function of the length L for different spiral tubing cross sections.

The theory indicates that the shunt impedance decreases with increasing tubing diameter d and that an optimum value for the ratio of pitch s to wire diameter d of s/d ≈ 2 should be chosen. The limits imposed by the required stability of the spirals and the cooling water flow thus become clear.

Fig. 5 shows the parameter dependance of the shunt impedance if only one parameter is varied, referred to the optimized value of η = 38,2 MΩ for a spiral with L = 20 cm, d = 2.0 cm, s = 4.0 cm, gapwidth g = 2.5 cm, and drift tube length 5 cm for a frequency of 108.5 MHz. The thick tubing was chosen to have sufficient stability, which varies roughly proportional to d^4 as will be shown later in the experimental data.

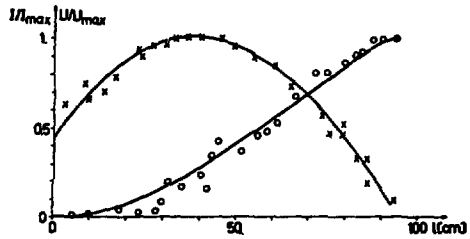

Fig. 2 Current and voltage distribution along the spiral tubing

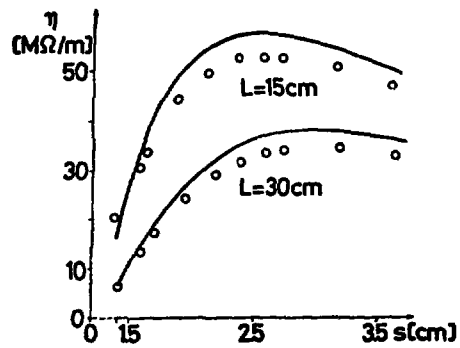

Fig. 3 Shunt impedance η of spirals as function of the pitch s. Tubing diameter 1.2 cm, frequency 100 MHz, tank diameter 35 cm

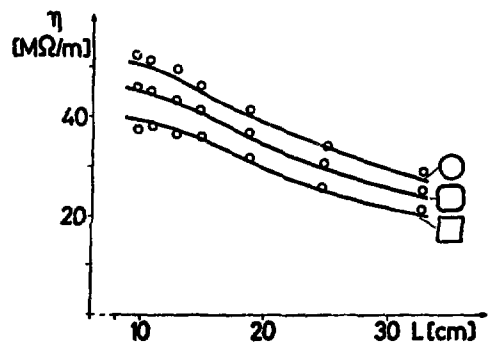

Fig. 4 Shunt impedance η of spirals as function of the tank length L for different spiral cross sections. Tubing diameter 2.0 cm, tank diameter 35 cm, pitch s 4.0 cm

Table 1 shows the parameters and the shunt impedances for the ten spiral resonators, which had been studied in high power tests. The measured and calculated values of the shunt impedance η are in very good accordance. Values for η up to 50 MΩ/m and for $R_p = \eta \cdot L$ up to 8 MΩ were measured.

High power tests

A number of high power tests was made to investigate the operating stability of the spiral at field levels necessary in working accelerators and to test the sizing and the mechanical construction of the spiral, the rf coupling, the drift tubes, the tank dimensions, and the cooling system.

For these tests a transmitter was used which delivers a rf power up to N = 100 kW (duty cycle 100 %), resp. N = 200 kW (duty cycle 25 %) at a frequency of 108.5 MHz. The rf power is fed in by a 50 Ω-coaxial line and a small watercooled loop. Impedance matching better than 50 dB could be reached by adjusting the angle between the loop and the spiral plane. The cooling of the spiral conductor and the drift tube was provided by an additional tube inside the spiral as indicated in fig. 6 (except spirals IV- VII which are constructed of two parallel tubes brazed together).

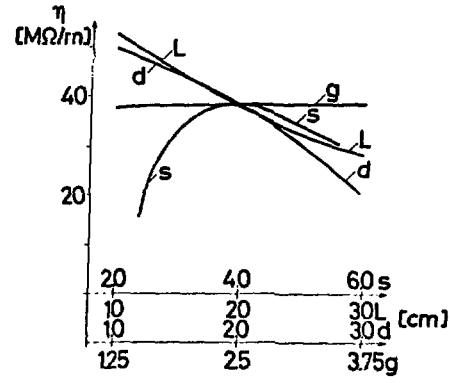

Fig. 5 Shunt impedance η of spirals referred to an optimized spiral if only one parameter is varied

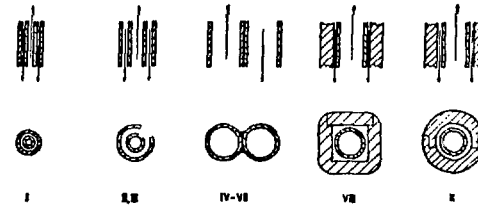

Fig. 6 Cross sections of the spiral tubing for the spiral resonators tested

Table 1

Parameters of the spiral resonators

No. of the spiral	tank length L [cm]	tank radius [cm]	pitch s [cm]	spiral tubing diam. d [cm]	gap width g [cm]	Q_o	R_p [MΩ]	η [MΩ/m]	η_{eff} [MΩ/m]	opt. particle energy [MeV/N]	theory R_p [MΩ]	theory η [MΩ/m]
I	14.7	12.0	1.4	0.8	5.85	3030	7.4	50.1	30.4	2.3	7.7	52.5
II	14.7	12.0	2.4	1.2	5.85	2650	7.4	49.9	30.3	2.3	7.3	49.7
III	13.4	12.5	1.7	1.2	2.2	2695	5.1	38.4	30.6	0.8	5.3	39.8
IV	27.0	17.5	3.1	2 x 1.2	8.5	4430	8.1	29.9	20.1	4.5	8.1	29.8
V	20.7	17.5	3.1	2 x 1.2	5.8	4270	7.15	34.5	24.3	2.75	7.5	36.3
VI	18.0	17.5	3.1	2 x 1.2	4.0	4125	7.05	39.2	28.6	2.0	7.15	39.8
VII	16.2	17.5	3.1	2 x 1.2	3.1	4030	7.0	43.0	33.3	1.8	6.9	42.5
VIII	27.5	17.5	4.5	0.5 cm edge radius 2.0 x 2.0	8.25	4275	6.6	24.0	17.3	5.0	6.7	24.5
IX	18.0	17.5	4.5	2.0 x 2.0	3.5	4330	6.0	33.5	27.6	2.25	5.9	32.9
X	20.0	17.5	4.0	2.0	2.5	4810	7.7	38.8	31.8	2.0	7.6	38.2

Fig. 7 shows a general layout of the test devices. Ten spiral resonators were tested at rf power levels of 40 kW or more. Each of them has to be tuned up with power levels of about 20 kW at small duty cycle for some hours. After this conditioning the resonators could also be operated at very small power levels without multipactoring. The first spirals with thin tubing diameter showed a large frequency shift due to radiation pressure and amplitude modulation of the tank pick-up signal. These oscillations are favoured by the fact that the spirals can only be fixed mechanically at the grounding point. An additional effect comes from the current maximum on the first winding as shown in fig. 2. At high field levels such spirals can only be operated with sophisticated and expensive control devices.

Therefore we increased the tubing diameter and wound the spirals with a greater pitch to improve stability. Table 2 shows the results of the high power tests. In comparison with spirals I - III, the spirals IV - VII have a smaller static frequency shift Δf_{stat}, which indicates a light increase with smaller gap widths g and tank lengths L. These tests were made in a tank with movable end plates. Thus tank and spiral geometry remained unchanged, except the spiral had to be shortened to give the proper resonance frequency of 108.5 MHz.

At levels of about 50 kW (duty cycle 100 %) the static frequency shift nevertheless had values of more than 100 kHz, which is clearly more than the bandwidth. Under such operating conditions one has "overhanging" resonance curves and thereby needs sophisticated control devices. For further improvement of the stability the next spirals were milled out of a copper plate and brazed together as indicated in fig. 6. With this method the spirals could be made with a tubing diameter of 20 mm and a wall thickness of 4 mm. The experiments showed a very small frequency shift of less than 0.2 kHz/kW, and the tendency to vibrations was considerably reduced.

These milled spirals could be run in pulsed operation even without any control loop with a phase ripple between spiral pick-up and power line of less than 1 ° at a rf power of 20 kW (duty cycle 20 %). With our control loop (bandwidth 25 kHz) the spiral resonators VIII and IX can be operated with a phase ripple between 0.1 ° and 1 ° dependent on the rf input power level. Only if the pulse repetition rate equals a mechanical resonance up to 10° were measured.

Fig. 8 shows a view of spiral resonator X with rf coupling loop and tuning ball.

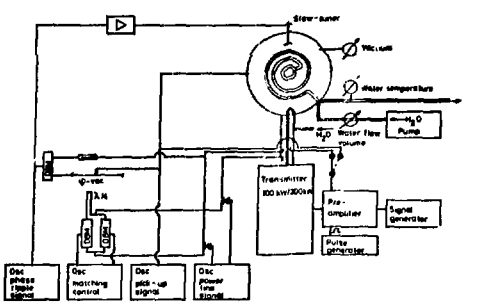

Fig. 7 Block diagram of the high power test arrangement

Table 2

Results of high power tests on spiral resonators

No. of the spiral	duty cycle 100 % N_{max} [kW]	$E_{z\,max}$ [MV/m]	ΔU_{eff} [MV]	duty cycle 25 % N_{max} [kW]	$E_{z\,max}$ [MV/m]	ΔU_{eff} [MV]	static frequency shift $-\Delta f_{stat}$ [kHz/kW]
I	48	7.5	0.46	123	12.1	0.74	57
II	49	7.6	0.46	158	13.5	0.84	4.5
III	38	9.2	0.40	117	16.1	0.69	20
IV	41	5.1	0.47	157	10.1	0.93	2.1
V	40	5.2	0.45	164	10.4	0.91	2.2
VI	40	5.8	0.45	150	11.3	0.88	2.5
VII	40	7.2	0.46	150	14.0	0.90	3.2
VIII	65	5.6	0.64	165	7.9	0.88	< 0.2
IX	80	9.2	0.68	160	13.0	0.96	< 0.2

Fig. 8 View of spiral resonator X

Spiral X is under test now and rf power up to 150 kW in pulsed operation has already been achieved. This spiral has a higher shunt impedance and preliminary results indicate that their stability is as good as of spirals VIII and IX.

As can be seen in Table 2 rf power levels up to 85 kW (duty cycle 100 %) and 165 kW (duty cycle 25 %) and axial field strength up to 16 MV/m could be obtained. The corresponding voltage gain was 0.68 MV, resp. 0.96 MV per section.

Possible Applications

These good results show that such spiral resonators are well suited for post acceleration of heavy ions with a MP Tandem as injector. For example a chain of 30 of such resonators, which are individually phased, provide a voltage gain of 15 MV with a total length of about 7 m (with integrated quadrupoles) and a power consumption of only 40 kW per section.

This voltage gain leads to final energies of 6 MeV/N for Br^{+26} and of 12 MeV/N for C^{+6}, using the general layout and the data of the Tandem machine described in[10]. Fig. 9 shows a possible arrangement for such a resonator chain. The acceptance with one singulet quadrupole per cavity is 3.0 cm mrad (normalized), using only one singulet for every second cavity 1.3 cm mrad are calculated. Further details and other focusing methods see [11].

Since the cavities can be operated at much higher field levels than assumed here, the voltage gain of the post accelerator can be increased up to a factor of two by running with higher rf power in pulsed operation. Other possible applications of spiral resonators are their use for buncher, rebuncher, and for injector linacs for synchrotrons.

Conclusions

The results of calculations and experiments show that spirals can be built with high shunt impedance and very good stability. In CW operation field strengths on axis up to 9.2 MV/m (16.1 MV/m, duty cycle 25 %) corresponding to voltage gains per section of 0.68 MV (0.96 MV) were achieved. With such stable spirals oscillations and static frequency shift can be supressed almost totally. With 100 % duty cycle phase ripple could be made smaller than 1.0 ° for a rf power of 80 kW.

Increasing the mechanical stability of the spirals causes a drop in shunt impedance but the operation range can be shifted to very high power levels without high control device requirements. The high shunt impedance and the good stability lead to obvious advantages compared to short

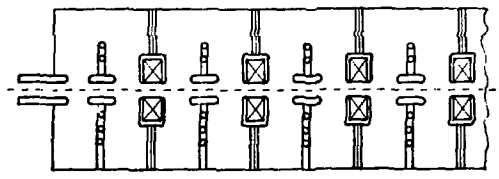

Fig. 9 Block of spiral resonators

λ/2-helices in the energy range up to 5 MeV/N (above 5 MeV/N helices have comparable shunt impedances and are as stable as spirals, because they can be made of thick tubing, too[12]). The construction of the spiral, the tank, the water-cooled rf coupling with the rubber sealed alumina disc, and the slow tuning device are well proved, so that we now have spiral resonators, which are adaptable for use in modular assemblies of independently phased resonator chains, as heavy ion post accelerators or injectors into synchrotrons for variable charge to mass ratio, or buncher and rebuncher cavities.

Acknowledgements

The authors would like to express their gratitude to K.-H. Buchberger, W. Caspar, Dr. H. Deitinghoff, T. Harji, G. Hausen, J. Krause, W. Rohrbach, H. Stöcker for valuable help.

Work supported by the Bundesministerium für Forschung und Technologie.

Computations were done at the Hochschulrechenzentrum, Universität Frankfurt/M.

References

[1] G.J. Dick and K.W. Shepard, Appl. Physics Lett. 24, 40 (1974).

[2] R.H. Stokes and D.D. Armstrong LA-5856 (1975).

[3] D.D. Armstrong, P.J. Bendt, B.H.Erkkila, J.S. Lunsford, J.P. Shipley, R.H. Stokes, J. Sutton, Part. Acc. 6, 175 (1975).

[4] A. Gamp, M. Glaser, G. Ihmels, E. Jaeschke, R. Repnow, DPG-Frühjahrstagung Baden (1976).

[5] A. Schempp, H. Klein, Nucl. Instr. Meth. 135, 409 (1976).

[6] A. Schempp, Thesis (Univ. Frankfurt/M., 1973).

[7] A. Schempp, H. Klein, Nucl. Instr. Meth. 136, 29 (1976).

[8] W. Rohrbach, A. Schempp, Univ. Frankfurt/M., Int. Rep. 75-11.

[9] O. Siart, Thesis (Univ. Frankfurt/M., 1970).

[10] H. Deitinghoff, H. Klein, M. Kuntze, J. E. Vetter, E. Jaeschke, R. Repnow, KFK-Bericht 2141 (1975),GSK Karlsruhe

[11] H. Deitinghoff, P. Junior, H. Klein, this conference.

[12] A. Schempp, P. Feigl, H. Klein, GSI-Bericht PB-4-75,(1975) Darmstadt

DISCUSSION

D.A. Swenson, LASL: You gave the figures for the peak electric field on the axis, could you also give a figure for the average value of the electric field on the axis?

Schempp: We obtained average field strengths of up to 4.2 MV/m in cw operation and 5.5 MV/m in pulsed operation.